

^2H NMR Evidence for the Formation of Random Mesh Phases in Nonionic Surfactant–Water Systems

Magdalena Bacia,^{*,†} Ulf Olsson,[‡] Marc S. Leaver,^{†,§} and Michael C. Holmes[†]

Department of Physics, Astronomy and Mathematics, Center For Materials Science, University of Central Lancashire, Preston, PR1 2HE, Lancashire, U.K., and Department of Physical Chemistry 1, Center for Chemistry and Chemical Engineering, Lund University, P.O. Box 124, SE-221 00 Lund, Sweden

Received: February 22, 2006; In Final Form: March 21, 2006

Random mesh phases share many common features with the classical lamellar phase in that they are layered phases; but crucially, they possess nonuniform interfacial curvature, since the lamellae are pierced by water-filled pores. The introduction of curvature into the lamellae has been posited as a transitional precursor for other lyotropic phases. In this paper, we show that simple ^2H nuclear magnetic resonance (NMR) experiments provide strong indication for the formation of the random mesh phase and the NMR data correlate well with literature results from small-angle X-ray scattering. The thermal evolution of the recorded quadrupolar splitting ($\Delta\nu_Q$) is monitored within the lamellar phase of two nonionic surfactants, C_{16}E_6 and C_{12}E_5 , as the samples are cooled or heated, and a marked and reversible change in the evolution of $\Delta\nu_Q$ is observed. Data from heavy water and deuterium labeled surfactant show the same temperature dependence and consequently report on the same structural changes with temperature. The formation of the random mesh phase is quantified in terms of an effective order parameter that is unity in the classical lamellar phase and takes values of <1 in the random mesh phase, reaching 0.6 at lower temperatures.

1. Introduction

Mesh phases are structurally very similar to the classical lamellar phase, since they consist of stacked surfactant bilayers.^{1–7} However, they possess water-filled pores within the bilayers. In the random mesh phase, the positions of the pores are uncorrelated between and within the layers.^{7–9} Even though the symmetry of the lamellar and random mesh phases is identical, the bilayer microstructure is significantly different, making difficult a clear discrimination between these phases. While the number of observations of the random mesh phase is increasing, the complexity of phase characterization impedes further reports of such phases.

The random mesh phase or “porous” lamellar phase has been shown to exist in a number of self-assembly systems.^{4–6,10–15} The phase diagrams of certain nonionic alkyloligoethylene oxide-type surfactants (C_nE_m) in water exhibit such phases. These surfactants are useful in this study, since their monolayer spontaneous curvature is strongly dependent on temperature variation and thus facilitates a controlled investigation of the evolution of the curvature of the surfactant–water interface in such systems.¹⁶ In nonionic surfactant liquid crystalline phases, at fixed surfactant-to-water ratios, the interfacial curvature is

tuned by the temperature-induced variation in the hydration of the polyoxyethylene oxide headgroups.^{17,18} At high temperatures, the headgroups tend to dehydrate, favoring phases that possess low interfacial curvature; while at lower temperatures, the headgroups are more hydrated, thereby occupying a larger area in the interfacial region and favoring phases with increased interfacial curvature. In certain systems, the “lamellar region” has been shown to consist of two phases: a high-temperature lamellar phase, which transforms into a random mesh phase at lower temperatures. Extensive characterization of both the phase behavior and the structure of the random mesh phase is available for the C_{16}E_6 and C_{12}E_5 (in H_2O or $^2\text{H}_2\text{O}$) systems.^{6,7,10,11,19,20}

In this letter, we briefly review the characterization of the random mesh phase and demonstrate that simple deuterium nuclear magnetic resonance, ^2H NMR, on deuterated water ($^2\text{H}_2\text{O}$) in such lyotropic phases is extremely sensitive to the changes in the local microstructure at the transition from the lamellar to random mesh phase, thereby providing a tool to rapidly identify the existence regions of such phases with significantly greater ease than previously. To achieve this, we compare the temperature evolution of the quadrupolar splitting ($\Delta\nu_Q$) obtained for α -deuterated $\text{C}_m\text{E}_n/\text{H}_2\text{O}$ systems with that for the $\text{C}_m\text{E}_n/^2\text{H}_2\text{O}$ systems. The results obtained from the α -deuterated C_{16}E_6 and C_{12}E_5 are more directly related to the local microstructure of the surfactant–water interface, since the signal is obtained from the α -carbon of the hydrophobic surfactant alkyl chain. However, here we show that the quadrupolar splitting from heavy water is directly proportional to the splitting from the α -deuterated surfactant, demonstrating

* For correspondence current address: Institut fuer Physikalische Chemie I, Universitaet zu Koeln, Luxemburger Str. 116, Koeln, D-50939, Germany. E-mail: magdalena.bacia@uni-koeln.de; Tel: +49 221 470 7336, Fax: +49 221 470 5104.

[†] University of Central Lancashire.

[‡] Lund University.

[§] Current address: St Mary's Catholic College, St Walburga's Road, Blackpool, Lancashire, FY3 7EQ, U.K.

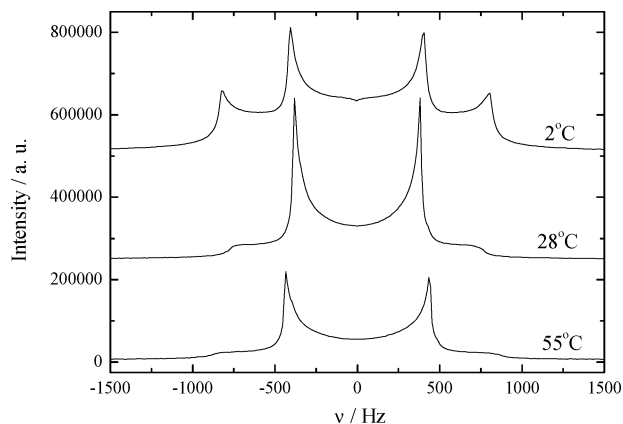


Figure 1. The quadrupolar nuclear magnetic resonance spectra recorded in the lamellar (55 °C), random mesh (28 °C), and hexagonal (2 °C) phases of a 57.41 wt % $C_{12}E_5$ sample in 2H_2O . All spectra are Pake powders, and the quadrupolar splitting ($\Delta\nu_Q$) is measured from the separation of the inner peaks in all cases.

that the heavy water splittings report on the same local order parameter describing the local curvature.

2. Materials and Methods

The surfactants hexaethylene glycol *n*-hexadecyl ether ($C_{16}E_6$) and pentaethylene glycol dodecyl ether ($C_{12}E_5$) were supplied by Nikko Chemical Co. Ltd., Tokyo, and had purities of $\geq 98\%$. The 2H_2O with $\geq 99.8\%$ atom 2H was supplied by Dr. Glaser AG, Basel. The α -deuterated nonionic surfactants $CH_3(CH_2)_{14}CD_2(OCH_2CH_2)_6OH$ ($C_{16}E_6$) and $CH_3(CH_2)_{10}CD_2(OCH_2CH_2)_5OH$ ($C_{12}E_5$) were synthesized by Synthelec, Lund, Sweden. All chemicals were used as received.

The 54 wt % $C_{16}E_6$ and 57.4 wt % $C_{12}E_5$ in 2H_2O samples were studied along with the homologous samples containing α -deuterated surfactant (i.e., mole ratio C_mE_n to α -deuterated C_mE_n of 5:1) prepared in Millipore H_2O having exactly the same surfactant-to-water mole ratio, namely, 56.6 wt % $C_{16}E_6$ and 60 wt % $C_{12}E_5$. For $C_{16}E_6$, the sample concentration was chosen, since it is in the middle of the random mesh phase stability region of the $C_{16}E_6$ phase diagram.⁶ For $C_{12}E_5$, the sample concentration was chosen to correspond to a sample studied by Imai et al.¹⁰ and also, as in the case of the $C_{16}E_6$ surfactant system, it possesses both a bicontinuous cubic phase and a hexagonal phase at lower temperature.

2H NMR experiments were carried out on a Bruker DMX100 NMR spectrometer operating at 15.67 MHz in a 2.35 T magnetic field. The quadrupolar splitting values in the lamellar and random mesh phases were recorded using the quadrupolar-echo sequence. The temperature of the sample was achieved and maintained using an airflow system, to an accuracy of ± 1 °C.

3. Results and Discussion

The transition from the classical lamellar phase to the random mesh is marked by subtle changes in the observed optical texture, individual NMR spectra, and small-angle X-ray scattering, but clear changes in the evolution of the observed 2H NMR quadrupolar splitting.^{6,10,11} Transition temperatures are a few degrees higher in H_2O compared with 2H_2O . This isotope dependence is a common feature of this kind of surfactant.¹⁹

Figure 1 shows the 2H NMR spectra obtained from 2H_2O in the lamellar, random mesh, and hexagonal phases of a 57.41 wt % $C_{12}E_5$ sample as it is cooled. As can be seen, the change of the spectra over ~ 50 °C is small, reflecting mainly a change in the director orientations within the phases. However, if the

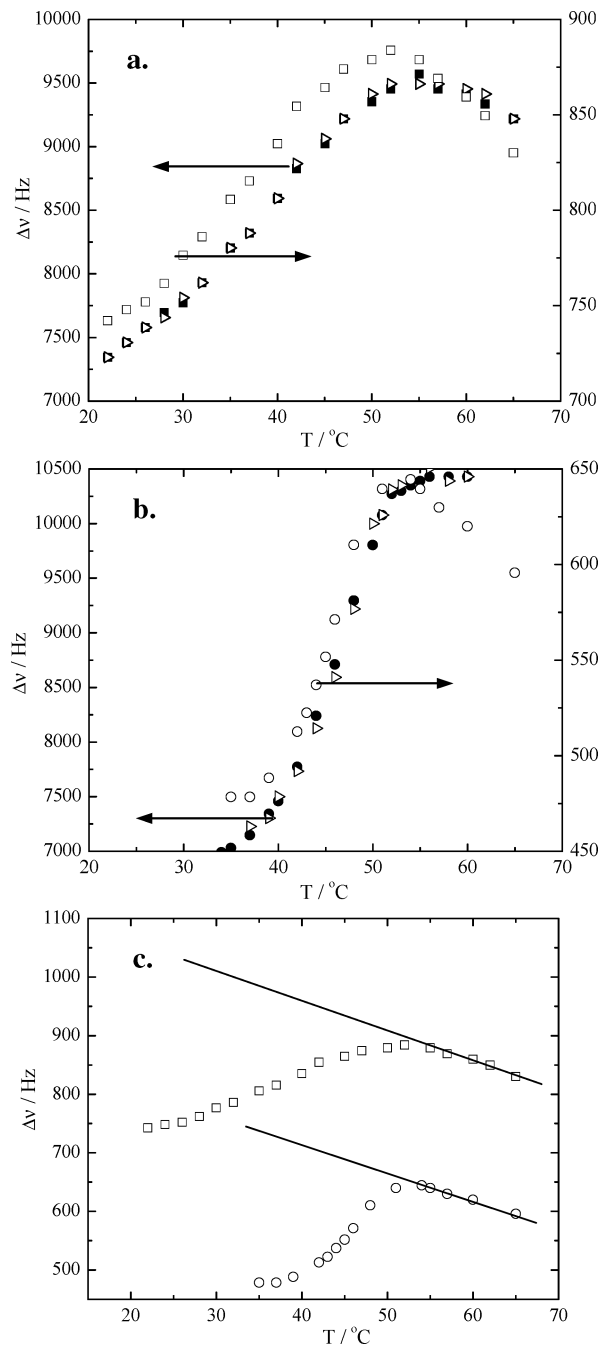


Figure 2. 2H NMR quadrupolar splitting ($\Delta\nu_Q$) evolution: open symbols stand for the $\Delta\nu_Q$ values measured on cooling for the “perturbed” 2H_2O molecules; filled symbols stand for the $\Delta\nu_Q$ recorded from α -deuterated surfactants (i.e., filled triangles are the data recorded on heating, and they overlap perfectly with the filled circles that represent the data recorded on cooling). The arrows are a guide for the eye pointing to the relevant $\Delta\nu_Q$ axis used to plot the data. Parts a and b illustrate the experimental data obtained from the $C_{12}E_5$ and $C_{16}E_6$ systems, respectively. Note that, in both figures, in the evolution of $\Delta\nu_Q$ a “turnover” occurs at about 52 °C, and it is interpreted as an indication for the transition from the lamellar phase to the random mesh phase. The solid lines in part c, which are an extrapolation from high-temperature data, correspond to the predicted increase of the (reference-) quadrupolar splitting with decreasing temperature for the imperforated lamellar structure, for both systems $C_{12}E_5/^2H_2O$ (above) and $C_{16}E_6/^2H_2O$ (below).

evolution of $\Delta\nu_Q$ is monitored, it is possible to observe a “turnover” in the recorded behavior (see Figure 2). This maximum in the quadrupolar splitting at approximately 52 °C marks the boundary between the classical lamellar phase

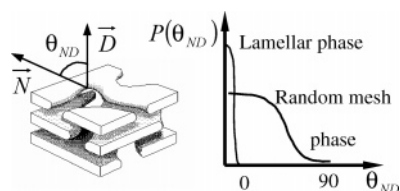


Figure 3. A schematic picture of the structural evolution of the phases formed upon cooling from the lamellar phase of $C_{12}E_5$ /water system. The insert illustrates the expected distribution function of local director orientations for the lamellar and random mesh phases.

structure and the random mesh phase. This identification of the transition temperature is in good agreement with SAXS data on the same system.

As it can be seen in Figure 2, the evolution of $\Delta\nu_Q$ and the “turnover” aspect are independent of whether the NMR is recorded directly from 2H attached to the α -carbon of the surfactant chain (directly monitoring the surfactant–water interface) or from 2H_2O partly perturbed by the interfaces. This shows clearly that the two “probes” are sensing identical microstructural changes, and the more easily available heavy water can safely be used to monitor the structural changes.

In the case of the deuterium-labeled surfactant, experiments were performed both upon heating and upon cooling, and both data sets are reported in Figure 2a,b. As can be seen, the data sets from heating and cooling overlap perfectly, demonstrating a very important fact, namely, that the structural changes monitored here are reversible and represent thermal equilibrium.

For all four samples outlined above, the evolution of $\Delta\nu_Q$ upon cooling from the lamellar phase (Figure 2) shows the characteristic “turnover” at approximately 52 °C.

Above 52 °C, within the lamellar phase, one can notice that $\Delta\nu_Q$ decreases with increasing temperature due to the trivial increase in thermal energy. However, below 52 °C, $\Delta\nu_Q$ decreases with decreasing temperature, indicating that the interfacial arrangement of surfactant molecules is changing significantly. If the phase would have been a classic lamellar phase, the order parameter would have stayed constant (i.e., $S = S_o$), and thus, the recorded $\Delta\nu_Q$ should have remained constant or slightly increased. In Figure 2c, we have made a linear extrapolation to lower temperatures of the high-temperature lamellar phase data, to serve as a reference for the quadrupolar splitting. Upon the formation of the random mesh phase, the formation and growth of pores introduces curvature into the lamellae, since pores’ edges have to be curved to restrict ingress of water into the hydrophobic cores.

Within the random mesh phase, the interfacial curvature is nonuniform, containing both flat and curved environments. Thus, the surfactant molecules are free to diffuse over the porous bilayers accessing both flat and curved environments, thereby experiencing an effective order parameter S_c , which is the average of the order parameter of both environments flat and curved. As pores are formed, the local structure director (\vec{N}) accesses a variety of orientations (θ_{ND}) with respect to the director of the lamellar phase (\vec{D}) (see Figure 3). Assuming threefold or higher symmetry, it is possible to define the effective order parameter S_c , which takes the form²¹

$$S_c = \frac{1}{2} \langle 3 \cos^2 \theta_{ND} - 1 \rangle \quad (1)$$

In the classical lamellar phase, the distribution function, $P(\theta_{ND})$, is narrow, with $\langle \theta_{ND} \rangle$ near 0. Once the random mesh phase is formed, $P(\theta_{ND})$ widens significantly, ensuring a concomitant

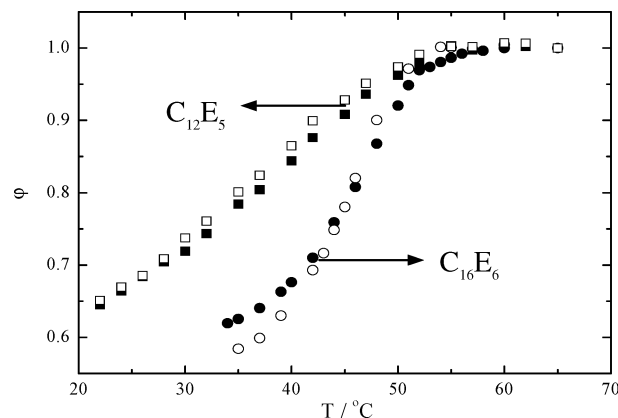


Figure 4. The rate of pore formation, φ (calculated using eq 2), for all surfactant systems studied. Open symbols represent φ calculated for “perturbed” 2H_2O molecules, while the filled symbols arise from the α -deuterated surfactants.

TABLE 1: Data Used in the Calculation of φ from Eq 2^a

system	ξ (Hz/°C)	$\Delta\nu_Q^o$ (Hz)
$C_{16}E_6/^2H_2O$	4.35	596
α -deuterated $C_{16}E_6/H_2O$	20.50	10430
$C_{12}E_5/^2H_2O$	4.70	830
α -deuterated $C_{12}E_5/H_2O$	32.60	9228

^a Here, ξ is the temperature compensation coefficient. $\Delta\nu_Q^o$ is the quadrupolar splitting measured for lamellar phase furthest from the transition to the random mesh phase.

decrease in the observed $\Delta\nu_Q$ of either 2H_2O or α -deuterated surfactant. This is shown schematically in Figure 3.

The continued decrease in $\Delta\nu_Q$ within the random mesh phase is a measure of the curved interface formation within the phase, indicating thus the rate of the pore formation, φ .

Using the quadrupolar splitting value recorded in the classical lamellar phase $\Delta\nu_Q^o$, it is possible to estimate the effect of temperature-induced hydration in the $C_nE_m/^2H_2O$ systems and surface area per molecule effects in the α -deuterated C_nE_m/H_2O systems, by calculating a temperature compensation coefficient per degree Celsius, ξ , assuming that the hydration and surface area effects are independent of the lyotropic phase.

This makes it possible to monitor the rate of the pore formation, φ

$$\varphi = \frac{S_c}{S_o} = \frac{\Delta\nu_Q^{\text{recorded}} \pm \xi \delta T}{\Delta\nu_Q^o} \quad (2)$$

where $\Delta\nu_Q^{\text{recorded}}$ is the quadrupolar splitting value measured, ξ is the temperature compensation coefficient, and δT is the temperature difference between the temperature at which φ is to be calculated and that of the highest lamellar phase recorded. In this case, $\Delta\nu_Q^o$ will always be that recorded at the highest temperature in the lamellar phase. The estimated values obtained for φ using eq 2 for the four systems studied are shown in Figure 4, with the data used to calculate φ displayed in Table 1.

Above 52 °C as the lamellar phase is entered, φ tends toward 1 for both $C_nE_m/^2H_2O$ and α -deuterated C_nE_m/H_2O systems, as would be expected. Below 52 °C in all samples studied, φ decreases from 1 to a value of about 0.6. For either surfactant, the evolution of φ is similar.

An additional experiment was carried out in the $C_{12}E_5$ systems. Here, the samples were crash-cooled into the hexagonal phase formed at 2 °C and $\Delta\nu_Q$ recorded. Rapid cooling was

necessary to avoid phase separation and the commensurate slow kinetics of reformation of the hexagonal phase from the cubic. The rapidly cooled sample gave a single Pake spectrum with $\Delta\nu_Q$ values of 7344 and 801 Hz, respectively, for the α -deuterated $C_{12}E_5$ and 2H_2O systems, having allowed 10 min for equilibration at 2 °C in the hexagonal phase prior to recording the spectra. The corresponding $\Delta\nu_Q$ values at 22 °C in the random mesh phase are 7344 and 742 Hz, respectively. While it is not possible to directly compare $\Delta\nu_Q$ between the random mesh phase and the hexagonal phase, the fact that they have similar $\Delta\nu_Q$ values could indicate that the hexagonal phase possesses similar curvature to that of the random mesh phase.

4. Conclusion

Deuterium NMR data from either heavy water or deuterium labeled surfactant can be conveniently used to monitor structural changes in surfactant systems such as the lamellar-to-random mesh transition. This transition is known to occur in the water- $C_{12}E_5$ and the water- $C_{16}E_6$ systems, but it is probably much more general. Our NMR data are in agreement with the $C_{16}E_6$ phase diagram of Fairhurst et al.⁶ and $C_{12}E_5$ data of Imai et al.^{10,11} and show that the two nonionic surfactant systems show similar trends when varying the temperature. Simple deuterium NMR experiments using heavy water can be a convenient tool when investigating the generality of the lamellar-to-random mesh transition.

Acknowledgment. This work was supported by the Swedish Research Council (VR).

References and Notes

- (1) Blackmore, E. S.; Tiddy, G. J. T. *J. Chem. Soc., Faraday Trans. 2* **1988**, *84*, 1115.
- (2) Fairhurst, C. E.; Fuller, S.; Gray, J.; Holmes, M. C.; Tiddy, G. J. T. In *Handbook of Liquid Crystals*; Demus, D., Gray, G. W., Goodby, J. W., Spiess, H. W., Vill, V., Eds.; Wiley-VCH: Germany, 1998; Vol. 3, Chapter VII.
- (3) Holmes, M. C. *Curr. Opin. Coll. Interface Sci.* **1998**, *3*, 485.
- (4) Gustafsson, J.; Oradd, G.; Lindblom, G.; Olsson, U.; Almgren, M. *Langmuir* **1997**, *13*, 852.
- (5) Gustafsson, J.; Oradd, G.; Nyden, M.; Hansson, P.; Almgren, M. *Langmuir* **1998**, *14*, 4987.
- (6) Fairhurst, C. E.; Holmes, M. C.; Leaver, M. S. *Langmuir* **1997**, *13*, 4964.
- (7) Fogden, A. S.; Fairhurst, C. E.; Holmes, M. C.; Leaver, M. S. *Langmuir* **2001**, *17*, 35.
- (8) Fogden, A. S.; Stenluka, M.; Fairhurst, C. E.; Holmes, M. C.; Leaver, M. S. *Prog. Colloid Polym. Sci.* **1998**, *108*, 129.
- (9) Almgren, M. *Aust. J. Chem.* **2003**, *56*, 959.
- (10) Imai, M.; Saeki, A.; Teramoto, T.; Kawaguchi, A.; Nakaya, K.; Kato, T.; Ito, K. *J. Chem. Phys.* **2001**, *115* (22), 10525.
- (11) Imai, M.; Sakai, K.; Kikuchi, M.; Nakaya, K.; Saeki, A.; Teramoto, T. *J. Chem. Phys.* **2005**, *122*, 214906.
- (12) Puntambekar, S.; Holmes, M. C.; Leaver, M. S. *Liq. Cryst.* **2000**, *27* (6), 743.
- (13) Funari, S. S.; Holmes, M. C.; Tiddy, G. J. T. *J. Phys. Chem.* **1994**, *98*, 3015.
- (14) Almdal, K.; Bates, F. S.; Mortensen, K. *J. Chem. Phys.* **1992**, *96*, 9122.
- (15) Vigild, M. E.; Almdal, K.; Mortensen, K.; Hamley, I. W.; Fairclough, J. P. A.; Ryan, A. J. *Macromolecules* **1998**, *31*, 5702.
- (16) Evans, D. F.; Wennerström, H. *The Colloidal Domain where Physics, Chemistry, Biology and Technology Meet*, 2nd ed.; Wiley-VCH: New York, 1999.
- (17) Andersson, M.; Karlström, G. *J. Phys. Chem.* **1985**, *89*, 4957.
- (18) Karlström, G. *J. Phys. Chem.* **1985**, *89*, 4962.
- (19) Strey, R.; Schomäcker, R.; Roux, D.; Nallet, F.; Olsson, U. *J. Chem. Soc., Faraday Trans. 1* **1990**, *86*, 2253.
- (20) Rendall, K.; Tiddy, G. J. T. *J. Chem. Soc., Faraday Trans. 1* **1984**, *80*, 3339.
- (21) Halle, B.; Wennerström, H. *J. Chem. Phys.* **1981**, *75* (4), 1928.